Wireless V2X Communication Testbed for Connected, Cooperative and Automated Mobility

Anja Dakić[1], Benjamin Rainer[1], Peter Priller[2], Guo Nan[3], Anamarija Momić[2], Xiaochun Ye[3], Thomas Zemen[1]

[1]AIT Austrian Institute of Technology GmbH, Vienna, Austria
[2]AVL List GmbH, Graz, Austria
[3]Institute of Computing Technology, CAS, Bejing, China
Email: anja.dakic@ait.ac.at

***Abstract*—Connected cooperative and automated mobility (CCAM) benefits from reliable wireless vehicle-to-everything (V2X) communication links in safety-critical and time-sensitive situations. The ego vehicle's perception, primarily derived from LIDAR, RADAR, and camera data, is limited by the line-of-sight (LOS). Sensor information beyond the LOS can be acquired by reliable V2X communication links from other cooperative vehicles or infrastructure elements. We identify CCAM use cases for both real-world applications and test phases, which stand to gain from understanding spatial reliability regions for communication links. Frame error rate (FER) classes for these regions, from the perspective of the ego vehicle, are provided to aid decision-making for autonomous vehicles. We propose a testbed architecture for system validation, verification, and test scenario generation, which integrates FER prediction through a high-performance open-source computing reference framework (HOPE). Our study demonstrates that the measured FER within a city scenario closely aligns with the FER obtained via a hardware-in-the-loop (HiL) framework and a non-stationary geometry-based stochastic channel model (GSCM) that utilizes OpenStreetMap data enriched with event-specific static objects. We use the GSCM and the HiL framework to overcome the fundamental limits of estimating the FER in non-stationary scenarios. As a final demonstration of the HOPE framework, we achieve an $80\,\%$ accuracy in predicting the FER class.**

***Index Terms*—ADAS, autonomous vehicles, verification and validation, ViL, SiL, GSCM, FER prediction**

I. Introduction

The goal of connected cooperative and automated mobility (CCAM) [1] is to increase road safety and improve traffic management. An enabler for CCAM is vehicle-to-everything (V2X) communication. Besides serving as a means to exchange information, V2X communication can be regarded as an additional sensor, thus holding high relevance for advanced driver assistance systems (ADAS). V2X enriches the vehicle's perception, enhancing the data foundation for decision-making.

Autonomous vehicles (AVs) are typically equipped with various sensors, such as LIDAR, RADAR, and cameras. These sensors aim to provide AVs with information about their immediate surroundings, including the position and shape of nearby objects such as traffic signs, static obstacles, and other road users. AVs must detect object movement to predict their trajectories. However, all the aforementioned sensors can only provide information from the AV's perspective, rendering objects hidden from the vehicle's sensors undetectable.

V2X represents a promising approach to provide missing complementary information. In this context, other actors, such as vehicles or road infrastructure, broadcast information. To accomplish this, they utilize different standards for the physical layer, such as IEEE 802.11p, IEEE 802.11bd, LTE-V2X, or 5G-V2X [2]. The most critical information broadcasted includes a vehicle's position, direction, and velocity [3]. Some systems also share detected objects from their own perception [4]. An AV capable of receiving such information via V2X can utilize it to extend and complement its own awareness.

Exhaustive testing and validation are crucial to ensure that all elements of AVs function cohesively, resulting in successful performance across various scenarios. There are two possibilities for testing: i) drive tests with a fully equipped AV and ii) (scenario-based) closed vehicle-in-the-loop (ViL) tests. Testing and validating ADAS features requires numerous kilometers to be driven and tackling various challenging traffic scenarios [5]. Therefore, conducting drive tests is not feasible during the design and prototyping phase of ADAS features.

On the other hand, ViL tests can be applied in different development phases [6], and they are conducted in controlled environments with the ability to replicate critical scenarios. An example of a ViL testbed is shown in [7]. Here, ADAS features undergo testing in the form of ViL tests where the vehicle sensors are stimulated. The authors of [8] propose a simple software-in-the-loop (SiL) setup for testing and validating ADAS applications in a simulation environment based on Autoware [9] and CARLA [10]. Furthermore, some simulation testbeds also integrate the V2X communication link into the validation process. Combining different vehicle and traffic simulation platforms, the authors in [11] test vehicle performance using V2X communications for a motion planning problem.

However, one essential piece of information missing for this task is the local V2X communication channel quality/reliability and therefore, what kind of quality of service (QoS) can be expected for potential communication between the AV and other road users. While measuring and simulating wireless communication channel properties, such as delay and Doppler spread, is possible with sometimes substantial effort,

predicting these properties in real-time, especially with limited computing resources available in a vehicle, is highly anticipated. The same holds for the inverse problem: automotive testing, for example, in a DRIVINGCUBE [12] setup, requires realistic simulation of wireless communication in typical traffic scenarios. In order to address this missing information, in [13], we propose a methodology for predicting the frame error rate (FER) of V2X communication channels. The methodology in [13] is based on machine learning and requires channel state information to predict the FER at a desired location.

In summary, both for trustworthy sensor fusion within a vehicle and for realistic real-time simulation on testbeds, a fast and realistic computation of channel properties for V2X communication is needed. In this paper, we introduce a flexible validation and verification framework that integrates a closed-loop testbed, i.e., SiL or ViL, together with V2X communication. This framework enables us to obtain the FER for a target receiver (Rx) position by calculating the channel transfer function (CTF) sequence using a geometry-based stochastic channel model (GSCM), and then applying the machine learning model proposed in [13].

Scientific Contributions of the Paper:

- We propose a testbed for the validation and verification of ADAS and AV functionality that takes V2X communication into account. This testbed integrates FER prediction into its core through the high-performance open-source computing reference framework (HOPE), forming a foundation for generating test scenarios for the identified use cases.
- We present a GSCM that utilizes the OpenStreetMap (OSM) geometry enriched with event-specific static objects. We demonstrate the impact of additional objects on the FER by comparing the FER obtained by emulating the CTF from the GSCM with the FER measured on the road.
- We evaluate the neural network module of the HOPE framework for predicting the FER classes with the CTF from the presented GSCM, achieving a good match in the regions of very high and low FER, with a total accuracy of 80 %.

II. CCAM Use Cases

To demonstrate and analyze the impact of providing vehicles with real-time V2X communication reliability estimations, we utilize the illustrative example depicted in Fig. 1: an intersection controlled by a traffic light. Buildings along the streets significantly disrupt line-of-sight (LOS) connectivity. Here, we showcase exemplary regions with different FER ranges, which serve as a reliability measure. The ego car is traveling from south to north (bottom to top), while the other car is following a different trajectory. We assume all cars are equipped with an active CCAM system.

We consider two important use cases, each exemplified using Fig. 1 when appropriate. The first one is related to the usage of V2X communication in real-world scenarios, while the second one relates to test scenarios.

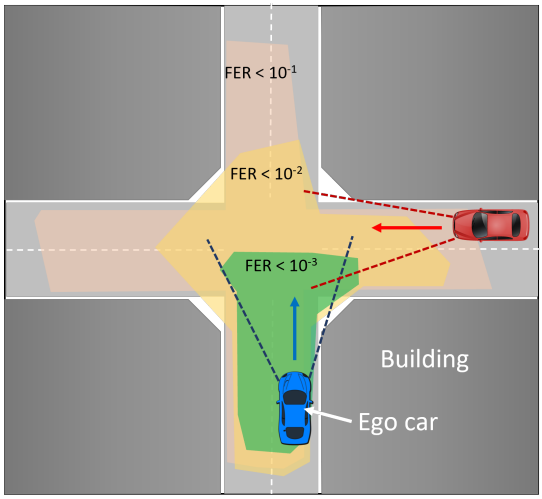

Fig. 1: Exemplary FER distribution at an urban intersection.

A. Use case 1: Prediction-guided Attention in Situations with Low Communication Reliability

In Fig. 1, the LOS between the two vehicles is obstructed by a building, resulting in a reduced signal-to-noise ratio (SNR). This leads to a high FER, indicating that only a few messages from vehicles in the vicinity of the second car are received correctly by the ego vehicle. Additionally, the ego vehicle's sensors are unable to detect other road users approaching from the left or right due to the blocked LOS by buildings. The high FER suggests that traffic-related V2X messages may not be received. Recognizing the high crash potential if a road user enters the intersection, the ego car reduces its velocity, thereby avoiding a potential accident cause.

B. Use case 2: Test Scenario Generation and High-fidelity Generation of V2X messages in Vehicle Test Environments

Verification and validation of AV in a vehicle testbed setup, such as the AVL DRIVINGCUBE described in [12], necessitates high-fidelity stimulation of vehicular sensors. Testing CCAM functionality thus requires the generation of V2X messages from simulated traffic participants, such as other vehicles, based on their virtual position and speed relative to the vehicle under test. Depending on the test goal, which could involve either testing if the CCAM functionality operates effectively under optimal conditions or exploring operational limits, test scenarios must be generated accordingly. Here, FER prediction enables a significant reduction in the number of test scenarios by selecting only those scenarios that meet the aforementioned test goals.

III. Testbed Architecture

We propose a testbed architecture that allows conducting both ViL/SiL and AV/ADAS testing with respect to V2X communication. Fig. 2 depicts the testbed architecture. The

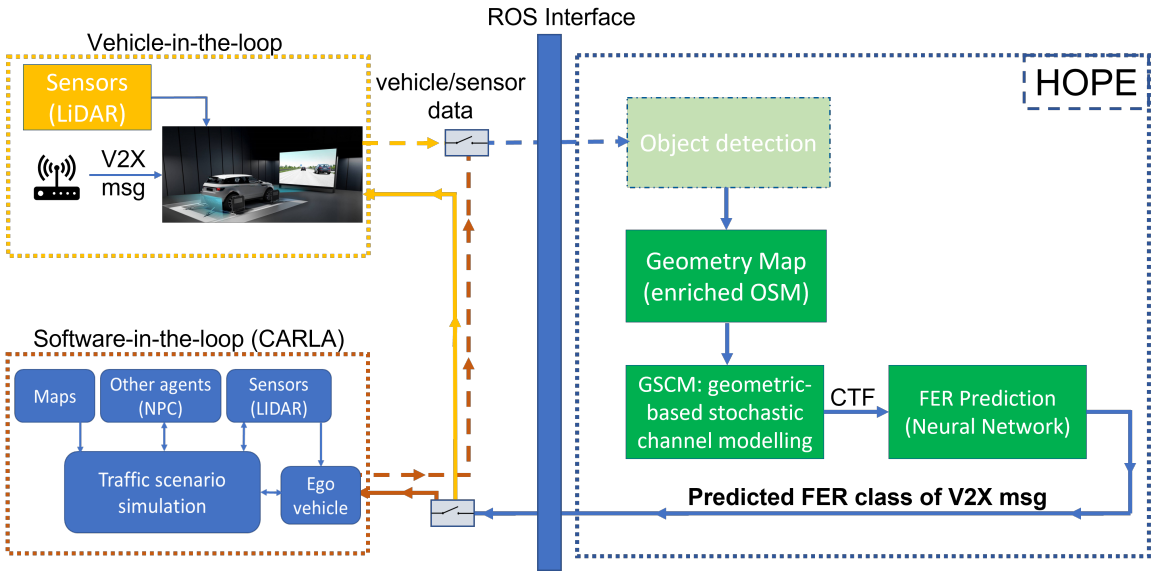

Fig. 2: Proposed testbed architecture

testbed does not distinguish between ViL and SiL and therefore, both ViL and SiL can be executed in our testbed as long as both adhere to the publish subscriber communication principle using the robot operating system (ROS) API [14]. The core of the testbed is represented by the HOPE framework with its modules, and in this paper, we focus on demonstrating and evaluating its usage. HOPE encapsulates the ROS communication principles and provides a module architecture for hot-swapping modules that process data published by the ViL or SiL system.

In this paper we use a GSCM with FER prediction on top of HOPE. The ViL/SiL provides sensor data and positions of the ego vehicles and other road users. HOPE then takes this data and routes it to its modules, which process the data. Sensor data are used for the object detection module and later on for enriching a geometry map. Using this map, together with the position of the transmitter (Tx) and Rx, we instantiate a GSCM which in turn provides us with the CTF. The GSCM is parameterized such that it provides CTFs similar to the measured ones. These CTFs are then used for predicting the FER class for the V2X communication assuming a specific communication standard, e.g., IEEE 802.11p.

A. HOPE

The high-performance open-source computing reference framework (HOPE) represents a framework that implements principles for interfacing with ROS-compliant software, essentially implementing wrappers for the publish-subscribe architecture defined in ROS (version 1 & 2). HOPE introduces a module system such that different modules can be loaded and may use the communication principles provided by HOPE to communicate with other modules orchestrated by HOPE, such as to send and receive data from external software. For our purpose, we implement four modules on top of HOPE:

- LIDAR object detection;
- Geometry map with dynamic updates;
- Geometry-based stochastic channel model;
- FER prediction.

In order to receive data from external software, each module can subscribe to ROS topics using the data broker available in HOPE. Modules may also publish data under their own topics, thereby allowing external software to receive data from modules running on top of the HOPE framework. HOPE is implemented in Python 3 and is available on https://github.com/parforme/RELEVANCE-HOPE.

B. Vehicle-in-the-Loop & Software-in-the-Loop Mode

On the lower left side of Fig. 2, an overview of the SiL test platform is presented. It is based on the industry-standard and open-source simulator CARLA. It encompasses various actors: vehicles, pedestrians, sensors, etc., along with maps that are amalgamated in user scripts, yielding diverse traffic test scenarios. Maps can be sourced from the default installation of CARLA, such as CARLA Town, or they can be imported from OpenStreetMap (OSM).

During simulations, the physical movement of the ego vehicle is simulated in CARLA, along with all sensors such as LIDAR, RADAR, and cameras. The sensor data is then published to HOPE and further utilized by the object detection module. The detected objects are incorporated into a geometry map, i.e., an OSM geometry. Based on the results, particularly on the predicted FER, further decisions and control of the ego vehicle are executed by CARLA. Other actors in the SiL or non-playable characters (NPC), which represent other road participants like vehicles and pedestrians, are also managed by CARLA. Furthermore, the CARLA API is utilized to retrieve object types and positions from the simulation, enabling the

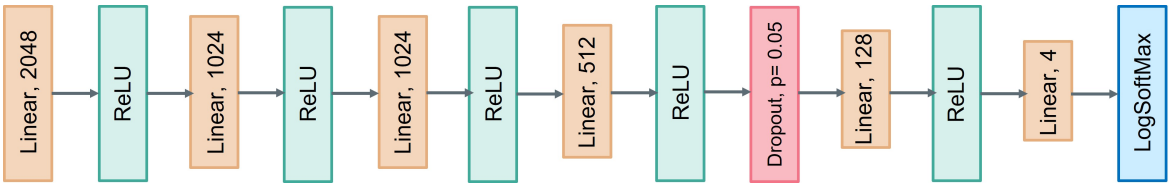

Fig. 3: DNN architecture introduced in [13]

feeding of this information into HOPE and subsequently to a channel prediction module to control the ego's behavior.

Additionally, at the top left side in Fig. 2, we observe the setup of the ViL. Here, the ego vehicle is represented by a ready-to-drive vehicle either on a chassis dynamometer or on a powertrain testbed (AVL's DRIVINGCUBE). The vehicle testbed stimulates relevant sensors, mimicking a realistic test environment. This includes one or more video screens for camera-based sensors and the generation of V2X messages of simulated road users. The computed FER prediction guides the testbed V2X modem in transmitting only those messages that would have been received in reality, as described in use case 2 in Section II.

C. Object Detection Module

Our proposed 3D object detection utilizes the PointVoxel-region based convolutional neural network (PV-RCNN) [15] and PointRCNN [16] methods separately from the open-source library OpenPCDet [17]. PV-RCNN combines voxel-based convolutional neural network and PointNet-based set abstractions, resulting in superior accuracy and runtime efficiency. By inputting LIDAR data into PV-RCNN, it automatically generates predicted 3D bounding boxes, object categories, and confidence scores. The detected objects are made available to HOPE as annotated bounding boxes via ROS and are further used by the GSCM.

D. FER Prediction

The prediction module is used to obtain the reliability of the V2X communication in terms of FER. It consists of two parts: (i) a numerical geometry-based radio channel model for an accurate representation of the non-stationary radio communication channels, and (ii) a machine learning-based prediction of the FER based on the CTF sequences per frame. In this work, the FER prediction is trained using a dataset with measured FER obtained by an IEEE 802.11p compliant V2X modem [18].

1) Geometry-Based Stochastic Channel Model: For modeling the radio communication channels we use a GSCM [19]. The geometry of the environment is imported from OSM [20], while the positions of the Tx and the Rx are obtained via GPS. The time-variant frequency response represents the summation of different contributions of the propagation paths: LOS between Tx and Rx, static discrete (SD) scatterers, e.g. traffic signs and lights, mobile discrete (MD) scatterers and diffuse (D) scatterers.

The OSM data lacks information about dynamic objects or recent infrastructure and environmental changes, such as parked or moving road vehicles or larger roadside installations (i.e., construction sites, etc.). These objects, as well as other missing objects and buildings, can be detected using data from vehicle sensors (i.e., LIDAR, RADAR, cameras). To detect dynamic and missing objects, we utilize the object detection module of HOPE (cf. Fig. 2).

2) Frame Error Rate Prediction: For the real-time prediction of the wireless V2X communication FER, we use a DNN. In general radio channels are non-stationary, but for a limited spatial region we may assume wide-sense stationarity (weak stationarity) [21], [22]. These regions are called stationarity regions.

As a specific machine learning algorithm, we implement a deep neural network (DNN). Assuming that a CTF sequence will be locally available information in the vehicle, we use it as an input vector for the DNN. For training the DNN, we utilize the CTF sequences generated from the GSCM described above. Since we are interested in obtaining reliability regions around the vehicle, we approach the FER prediction as a classification task. A detailed description of the FER prediction using the DNN, as well as the dataset collection, is provided in [13], and the architecture of the DNN is illustrated in Fig. 3.

IV. Testbed Evaluation

A. Geometry-Based Stochastic Channel Model

To illustrate the principle of the testbed and the impact of enriching geometry with observed static objects (by the ego vehicle) on the FER, we utilize already identified objects from a measurement campaign presented in [23]. We consider a V2V scenario where two cars approach each other and intend to share traffic information. Fig. 4 depicts the parsed OSM data without detected objects (left) and with detected objects (right), respectively.

We observe that in the original OSM, no SD scatterers are included. We identify the following additional objects: parked cars, city lamps, trees, and buildings, and incorporate them during runtime, for instance, via ROS messages conveying a description of the objects. We calibrate the GSCM using the radio channel data recorded by the AIT multi-node channel sounder [24] during the measurement campaign. The GSCM parameters for the propagation path computation and point scatterer distribution [25] are summarized in Table I. We model the deterministic amplitude of the LOS component as well as other scatterers using the log-distance path loss model [26],

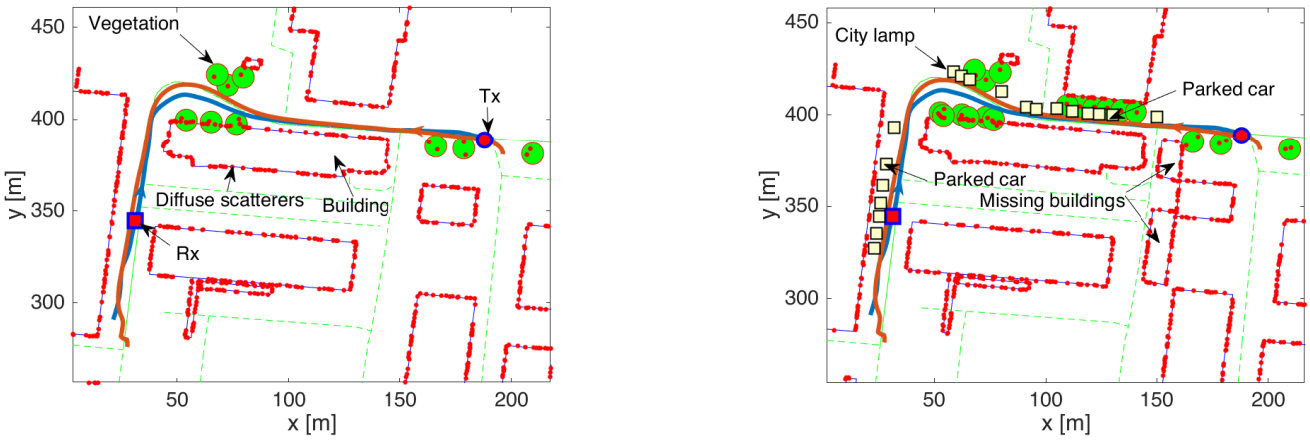

Fig. 4: Scenario map (a) geometry directly obtained by OSM data and (b) geometry enriched with detected objects.

where G_0 is the Rx gain at a reference distance, and n_p denotes the path loss exponent. For modeling the stochastic amplitude of the LOS component and SD scatterers we use a Gaussian function, with μ_σ as variance of the gain and d_c as the coherence distance. Diffuse scatterers are uniformly distributed and placed along buildings. To reduce the number of diffuse scatterers we employ the locality-sensitive hashing scheme adapted in [19].

Parameter	Description	LOS	SD	D
G_0 [dB]	reference Rx power	-1	-70	-10
n_p	path loss exponent	2.2	1.5	2.5
μ_σ [m]	mean variance of the stochastic amplitude gain	1	3.1	-
μ_c [m]	mean coherence distance	1.2	4.9	-
$d_\mathrm{c}^\mathrm{min}$ [m]	minimum coherence distance	1.4	1	-
χ_D [m^{-1}]	scatter point density	-	-	0.5
w_D [m]	maximum scatterer distance	-	-	0.5

TABLE I: GSCM parameters for the line-of-sight (LOS) component, static discrete scatterers (SD), and diffuse scatterers (D).

Fig. 5a depicts the power delay profile (PDP) and Doppler spectral density (DSD) from the measured CTF that are acquired with a sampling time of $T_\mathrm{S} = 500\,\mu$s [23]. In Fig. 5b the GSCM simulation with the OSM geometry is shown, where we notice strong components between approx. $5-10$ sec and again between approx. $32-38$ sec that are not present in the measurement data. We find that these components are caused by reflections/diffuse scattering mainly from the big building in the south of our environment (cf. Fig. 4a). Adding the additionally identified buildings, blocks these reflection paths (cf. Fig. 4b) and we obtain a better match between the measurement and the GSCM simulation in Fig. 5c.

B. FER Evaluation with Hardware-in-the-Loop Framework

The hardware-in-the-loop (HiL) framework connects a Tx and Rx via radio channel emulator [27]. The Tx and Rx are two IEEE 802.11p [18] compliant Cohda Wireless MK5 modems [28], exchanging ITS-G5 compliant data frames. These are the very same modems that have been used in the aforementioned measurement campaign [23].

The channel emulator needs a CTF sequence with a sampling time of 50 ns, which is obtained via interpolation, as explained in [27], either from the measured CTF or from the numerically computed CTF using the GSCM. The Tx modem is set to send 1500 frames per second with a length of 100 bytes. We choose a window of 1 s to evaluate the FER.

Fig. 6 plots the FER γ_meas versus time from the measured data, the FER $\gamma_\mathrm{GSCM,2}$ for the GSCM data using the OSM geometry (Fig. 4a), and the FER $\gamma_\mathrm{GSCM,1}$ using the OSM geometry with additional objects (Fig. 4b). We notice a good match in high and low FER regions. However, in the transition regions, from non-LOS (NLOS) to LOS and vice versa, we obtain a noticeable difference between the FER without additional/dynamic objects ($\gamma_\mathrm{GSCM,2}$). This is mainly due to missing buildings, highlighted in Fig. 4b, which block the signal between the Tx and Rx. This we can also see in Fig. 6 where $\gamma_\mathrm{GSCM,1}$ matches the measured FER also in transition regions.

Furthermore, we calculate the Jeffreys interval [29] as a 95% of the credible interval of the FER estimated by the HiL framework and the GSCM data with additional objects. We model the process of sending a frame as an independent Bernoulli process as we assume that only mission critical information is exchanged, only spanning a single frame. Therefore, the FER follows a binomial distribution, where the number of observations is the number of transmitted frames $\Psi = 1500$,

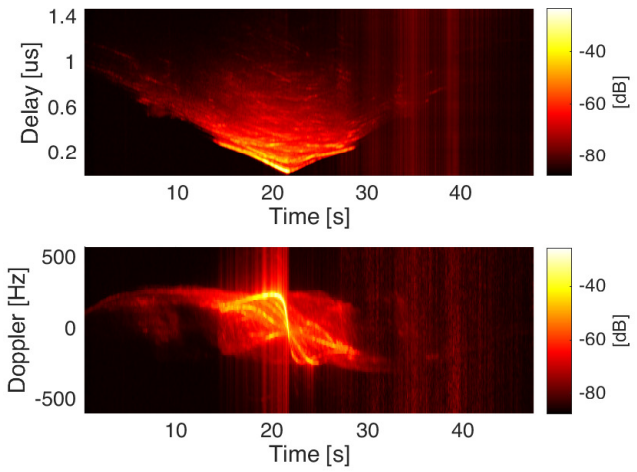

(a)

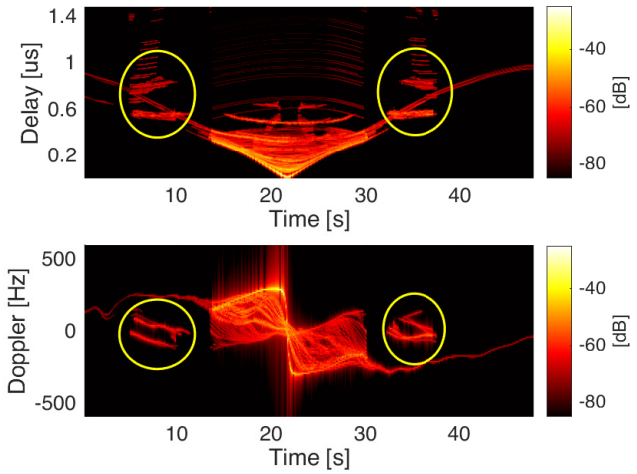

(b)

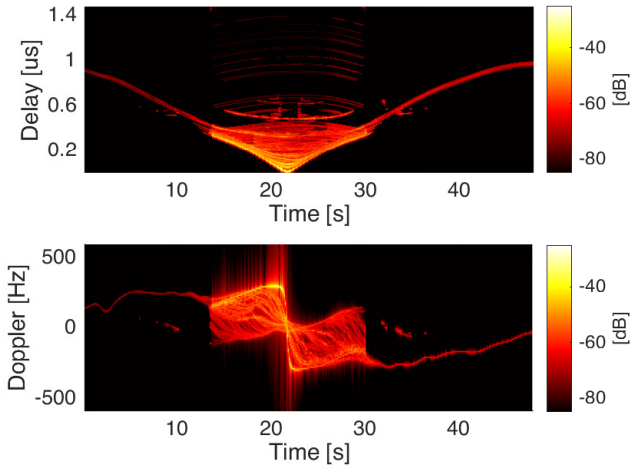

(c)

Fig. 5: Time-variant PDP and DSD: (a) Measurement, (b) GSCM simulation with OSM geometry, (c) GSCM simulations with OSM and additional detected objects.

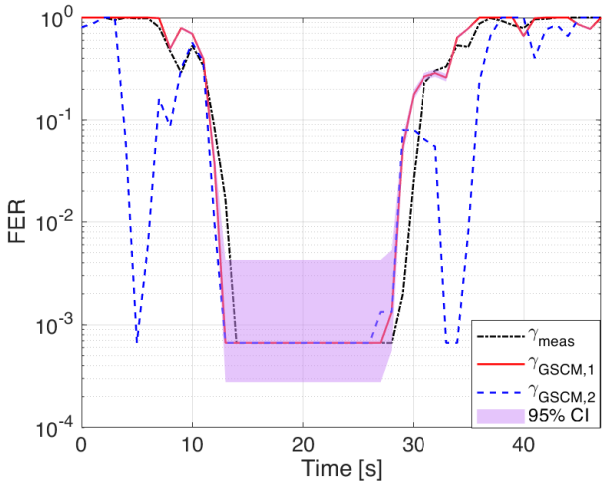

Fig. 6: FER comparison: FER γ_{meas} obtained directly on the road, FER $\gamma_{\text{GSCM,1}}$ obtained by emulating CTF from the GSCM in the case when all identified objects are included, and FER $\gamma_{\text{GSCM,2}}$ obtained by emulating CTF from the GSCM in the case when only objects from OSM are included. The violet region indicated the 95% confidence interval (CI) of the binomially distributed FER.

the number of successes is the number of lost frames L and the probability of successes is unknown. The results are shown as a shadowed area around $\gamma_{\text{GSCM,1}}$. We notice that Jeffreys interval is very small in the regions of the high FER, while it becomes wider when a small number of frames is lost, i.e. in the low FER regions.

C. DNN based FER evaluation

Before evaluating the FER obtained from the DNN, we briefly review the solution to the problem of measuring the FER in non-stationary communication channels, introduced in [13].

1) Frame Error Rate Measurement Method for Non-stationary Propagation Conditions: The spatial extent of stationarity regions D_{stat} is measured in a multiple of the wavelength $\lambda = c_0/f_{\text{C}}$ and depends on the propagation environment, here c_0 denotes the speed of light and f_{C} the carrier frequency. Given the vehicle velocity v we can compute the stationarity time $T_{\text{stat}} = D_{\text{stat}}/v$. For the chosen urban scenarios [30] found $T_{\text{stat}} < 100\,\text{ms}$.

The duration of a frame T_{frame} is defined by the bandwidth, bit rate, and frame length in terms of bytes. Hence, within a stationarity region only a finite number of frames

$$\Psi = \lfloor T_{\text{stat}}/T_{\text{frame}} \rfloor \tag{1}$$

can be transmitted. In [13] we introduced a methodology to overcome this fundamental limitation for non-stationary propagation conditions. A GSCM computes the CTF using a finite number P of propagation paths that are defined by path weight η_p, normalized Doppler shift ν_p and normalized

delay θ_p, with p being the path index $p \in \{1, \ldots, P-1\}$. Hence, keeping these propagation path parameters fixed we can extend the fading process of a stationary region as long as needed.

2) Evaluation Results: We use the FER obtained from the HiL framework as our ground truth. We extend each stationary region $s \in \{1, \ldots, S\}$ such that we can transmit $\Psi = 20000$ frames. The FER result $\gamma_{\text{GSCM},1}[s]$ versus time is presented by a solid line in Fig. 7. In order to evaluate the usefulness of the aforementioned methodology, we calculate the 95% confidence interval and show the results with the violet regions. With many more frames available for FER estimation, we can see that the confidence interval has improved in the low FER regions. Hence, we can overcome the fundamental limits of FER estimation within a non-stationary fading process.

Furthermore, we use the CTF sequence obtained by the GSCM for stationarity region s as input to our DNN. The output of the DNN is one of N classes for the predicted FER,

$$c_n := (x_{n,1},\, x_{n,2}], \tag{2}$$

where $n \in \{1, .., N\}$ defined as

- class 1: $c_1 := (0, 5 \cdot 10^{-4}]$,
- class 2: $c_2 := (5 \cdot 10^{-4}, 10^{-1}]$,
- class 3: $c_3 := (10^{-1}, 5 \cdot 10^{-1}]$,
- class 4: $c_4 := (5 \cdot 10^{-1}, 1]$.

We compute the accuracy of the DNN prediction

$$\mathrm{a}_k = \frac{M_k}{S\imath} \cdot 100\%\,, \tag{3}$$

for a time interval $[\Delta(k-1), \Delta k)$, with $\Delta = 1\,\mathrm{s}$ containing $S\imath = \Delta / T_{\text{stat}} = 10$ stationarity regions. Here, M_k denotes the number of correctly predicted classes per time interval. This result is depicted as colormap in Fig. 7.

We obtain a high accuracy in the region of very high FER (class 4) and of very low FER (class 1), while the accuracy in the NLOS/LOS transition regions is reduced. However, the DNN has been initially trained with data from a V2I scenario only. Therefore, the training data lacks CTFs which include those transition regions of V2V scenarios. We obtain an overall accuracy of 80 %. If we exclude the fast NLOS/LOS transitions we obtain an accuracy of 87 %.

V. Conclusion

In this paper, we describe a testbed that supports testing and validation of V2X communication for ViL and SiL ADAS testing and verification. We identify use cases where V2X communication plays a key role for ADAS. The testbed we propose allows the identification of critical scenarios reducing the number of test cases for scenario based testing and validation of ADAS features. Using the HOPE framework, we integrate a GSCM which uses OSM data enriched by dynamically detected objects from the vehicles' sensors. We evaluate the core of the testbed by showing that objects detected on the fly have a significant impact on the resulting FER. The results show that having an accurate geometry map is crucial for correctly modeling the radio channel and, therefore, obtaining a realistic FER. Finally, we include the FER prediction module in the evaluation of HOPE and obtain a total accuracy of 80 % with very high accuracy in the NLOS and the LOS cases even though the used DNN has been initially trained using data from a V2I scenario. This module enables us to extend the FER range and overcome the fundamental limits of FER analysis in non-stationary safety-critical scenarios.

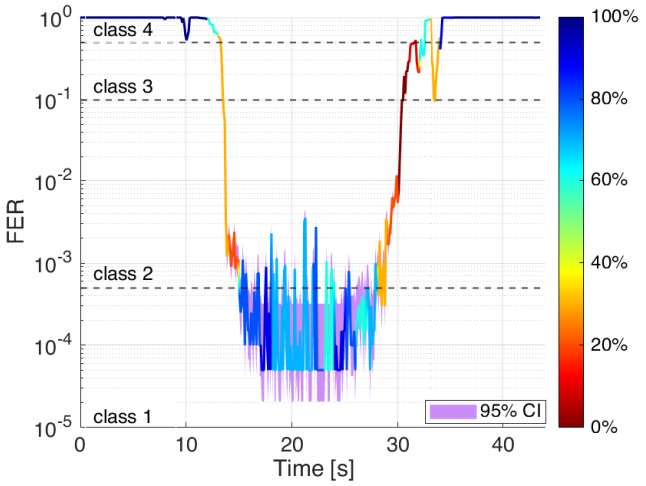

Fig. 7: Accuracy of the predicted FER per second. The prediction is done using the DNN and the CTFs generated from the GSCM with identified objects. The violet region indicated the 95% confidence interval (CI) of the binomially distributed FER.

VI. Acknowledgment

The authors of this work have received funding by the Austrian Research Promotion Agency (FFG) and the Austrian Ministry for Transport, Innovation and Technology (BMK) within the project RELEVANCE (881701) of the funding program transnational projects, by the European Commission within the European Union's Horizon 2020 research innovation program funding ECSEL Joint Undertaking project AI4CSM under Grant Agreement No. 101007326 within the project DEDICATE (Principal Scientist grant) at the AIT Austrian Institute of Technology, and from the ECSEL Joint Undertaking (JU) under grant agreement No. 101007350 (AIDOaRt project). The JU receives support from the European Union's Horizon 2020 research and innovation program and Sweden, Austria, Czech Republic, Finland, France, Italy, Spain.

References

[1] Cooperative, Connected and Automated Mobility. [Online]. Available: https://transport.ec.europa.eu/transport-themes/intelligent-transport-systems/cooperative-connected-and-automated-mobility-ccam_en

[2] W. Anwar, S. Dev, A. Kumar, N. Franchi, and G. Fettweis, "PHY abstraction techniques for V2X enabling technologies: Modeling and analysis," *IEEE Transactions on Vehicular Technology*, vol. 70, no. 2, pp. 1501–1517, 2021.

[3] ETSI, "ETSI EN 302 637-2 v1.4.1 - Intelligent transport systems (ITS); Vehicular communications; Basic set of applications; Part 2: Specification of cooperative awareness basic service," 2019.

[4] ——, "ETSI TR 103 562 v2.1.1 - Intelligent transport systems (ITS); Vehicular communications; Basic set of applications; Analysis of the collective perception service (CPS); Release 2," 2019.

[5] P. Junietz, W. Wachenfeld, K. Klonecki, and H. Winner, "Evaluation of different approaches to address safety validation of automated driving," in *21st International Conference on Intelligent Transportation Systems (ITSC)*, Hawai, USA, November 2018.

[6] S. Hallerbach, Y. Xia, U. Eberle, and F. Koester, "Simulation-based identification of critical scenarios for cooperative and automated vehicles," *SAE International Journal of Connected and Automated Vehicles*, vol. 1, no. 2018-01-1066, pp. 93–106, 2018.

[7] C. Galko, R. Rossi, and X. Savatier, "Vehicle-hardware-in-the-loop system for ADAS prototyping and validation," in *International Conference on Embedded Computer Systems: Architectures, Modeling, and Simulation (SAMOS XIV)*, Samos, Greece, July 2014, pp. 329–334.

[8] S. Stević, M. Krunić, M. Dragojević, and N. Kaprocki, "Development and validation of ADAS perception application in ROS environment integrated with CARLA simulator," in *27th Telecommunications Forum (TELFOR)*, Belgrade, Serbia, November 2019.

[9] Autoware-AI. [Online]. Available: https://github.com/Autoware-AI

[10] T.-K. Lee, T.-W. Wang, W.-X. Wu, Y.-C. Kuo, S.-H. Huang, G.-S. Wang, C.-Y. Lin, J.-J. Chen, and Y.-C. Tseng, "Building a V2X simulation framework for future autonomous driving," in *20th Asia-Pacific Network Operations and Management Symposium (APNOMS)*, Matsue, Japan, September 2019.

[11] S. K. Yetkin, M. Eren, N. Zengin, E. A. Rencüzoğullan, M. Tomruk, and H. Yılmaz, "V2X communication based system development: Application on intersection assist with co-simulation," in *IEEE 21st International Conference on Sciences and Techniques of Automatic Control and Computer Engineering (STA)*, Sousse, Tunisia, December 2022.

[12] AVL DRIVINGCUBE™. [Online]. Available: https://www.avl.com/en/testing-solutions/automated-and-connected-mobility-testing/avl-drivingcube

[13] A. Dakić, B. Rainer, M. Hofer, and T. Zemen, "Frame error rate prediction for non-stationary wireless vehicular communication links," in *IEEE International Symposium on Personal, Indoor and Mobile Radio Communications (PIMRC)*, Toronto, Canada, September 2023. [Online]. Available: https://arxiv.org/abs/2304.05743

[14] ROS documentation. [Online]. Available: http://wiki.ros.org/

[15] S. Shi, C. Guo, L. Jiang, Z. Wang, J. Shi, X. Wang, and H. Li, "PV-RCNN: point-voxel feature set abstraction for 3D object detection," in *IEEE/CVF Conference on Computer Vision and Pattern Recognition, (CVPR)*, virtual, June 2020.

[16] S. Shi, X. Wang, and H. Li, "PointRCNN: 3D object proposal generation and detection from point cloud," in *IEEE Conference on Computer Vision and Pattern Recognition, (CVPR)*, Long Beach, CA, USA, June 2019.

[17] OpenPCDet library. [Online]. Available: https://github.com/open-mmlab/OpenPCDet

[18] IEEE, "IEEE standard for information technology– local and metropolitan area networks– specific requirements– part 11: Wireless LAN medium access control (MAC) and physical layer (PHY) specifications amendment 6: Wireless access in vehicular environments," *IEEE Std 802.11p-2010*, 2010.

[19] B. Rainer, L. Bernadó, M. Hofer, S. Zelenbaba, D. Löschenbrand, A. Dakić, T. Zemen, P. Priller, X. Ye, and W. Li, "Optimized diffuse scattering selection for large area real-time geometry based stochastic modeling of vehicular communication links," in *IEEE MTT-S International Conference on Microwaves for Intelligent Mobility (ICMIM)*, July 2020.

[20] Openstreetmap. [Online]. Available: https://www.openstreetmap.org/#map=12/48.2677/14.3207

[21] L. Bernadó, T. Zemen, F. Tufvesson, A. F. Molisch, and C. F. Mecklenbräuker, "Delay and Doppler spreads of non-stationary vehicular channels for safety-relevant scenarios," *IEEE Transactions on Vehicular Technology*, vol. 63, no. 1, pp. 82–93, Jan 2014.

[22] L. Bernadó, T. Zemen, F. Tufvesson, A. F. Molisch, and C. F. Mecklenbräuker, "Time- and frequency-varying K-factor of non-stationary vehicular channels for safety-relevant scenarios," *IEEE Transactions on Intelligent Transportation Systems*, vol. 16, no. 2, pp. 1007–1017, 2015.

[23] B. Rainer, S. Zelenbaba, A. Dakić, M. Hofer, D. Löschenbrand, T. Zemen, X. Ye, G. Nan, S. Teschl, and P. Priller, "WiLi - vehicular wireless channel dataset enriched with LiDAR and Radar data," in *IEEE Global Communications Conference (GLOBECOM)*, Rio de Janeiro, Brazil, December 2022, pp. 4770–4775.

[24] S. Zelenbaba, B. Rainer, M. Hofer, D. Löschenbrand, A. Dakić, L. Bernadó, and T. Zemen, "Multi-node vehicular wireless channels: Measurements, large vehicle modeling, and hardware-in-the-loop evaluation," *IEEE Access*, vol. 9, pp. 112 439–112 453, 2021.

[25] J. Karedal, F. Tufvesson, N. Czink, A. Paier, C. Dumard, T. Zemen, C. F. Mecklenbrauker, and A. F. Molisch, "A geometry-based stochastic MIMO model for vehicle-to-vehicle communications," *IEEE Transactions on Wireless Communications*, vol. 8, no. 7, pp. 3646–3657, 2009.

[26] T. Rappaport, *Wireless communications: Principles and practice*, 2nd ed. Prentice Hall, 2002.

[27] A. Dakić, B. Rainer, M. Hofer, S. Zelenbaba, S. Teschl, G. Nan, P. Priller, X. Ye, and T. Zemen, "Hardware-in-the-loop framework for testing wireless V2X communication," in *IEEE Wireless Communications and Networking Conference (WCNC)*, Toronto, Canada, September 2023.

[28] Cohda Wireless MK5 OBU specifications. [Online]. Available: https://cohdawireless.com/solutions/hardware/mk5-obu/

[29] A. Agresti and B. A. Coull, "Approximate is better than "exact" for interval estimation of binomial proportions," *The American Statistician*, vol. 52, no. 2, pp. 119–126, 1998. [Online]. Available: https://doi.org/10.1080/00031305.1998.10480550

[30] L. Bernadó, T. Zemen, F. Tufvesson, A. F. Molisch, and C. F. Mecklenbräuker, "The (in-) validity of the WSSUS assumption in vehicular radio channels," in *IEEE 23rd International Symposium on Personal, Indoor and Mobile Radio Communications (PIMRC)*, Sydney, Australia, September 2012, pp. 1757–1762.